Contribution from the Institute for Inorganic Chemistry,
University of Witten/Herdecke, Stockumer Strasse 10, 5810 Witten, FRG

Mechanistic Information from a Volume Profile Treatment for the Complexation of Aquocobalamin (Vitamin B_{12a}) by Pyridine

G. Stochel[1] and R. van Eldik*

Received May 19, 1989

The complexation kinetics of aquocobalamin (vitamin B_{12a}) by pyridine was studied as a function of pyridine concentration, temperature, and pressure. The kinetic data equally well fit D and I_d mechanisms. The pressure dependence of the rate and equilibrium constants enables the construction of an overall reaction volume profile, from which it is concluded that both the forward complex formation and reverse aquation reactions proceed according to a limiting D mechanism.

Introduction

Substitution reactions of cobalamins have attracted significant attention from kineticists in recent years.[2-7] In the majority of these studies conventional kinetic techniques were employed, and kinetic data were reported as a function of concentration, pH, ionic strength, and solvent composition. The mechanistic interpretation of these data was restricted by the shortage of activation parameters for the rate-determining step, with the result that a differentiation between the operation of an I_d or a D mechanism for the substitution reactions of aquocobalamin (hereafter referred to as B_{12}–H_2O^+) was not possible.[2]

Our earlier experience with the successful application of high-pressure kinetic techniques in the elucidation of inorganic and organometallic reaction mechanisms[8,9] led us to study the pressure dependence of the anation of B_{12}–H_2O^+ by azide and several cyanoferrates.[10] The reported volumes of activation favor the operation of a D instead of I_d mechanism, although the interpretation of the data was complicated to some extent due to solvational contributions arising from charge neutralization during bond formation with anionic ligands. We have now completed a detailed study of the complexation of B_{12}–H_2O^+ by pyridine (py) and present here evidence for the operation of a limiting D mechanism. In addition, we report a volume profile analysis for the overall substitution process from which important conclusions regarding all mechanistic steps can be drawn.

Experimental Section

All experimental details, i.e. materials used and techniques employed, are identical with those reported elsewhere.[10] Preliminary kinetic measurements indicated that the substitution of B_{12}–H_2O^+ by py is independent of pH around 6.7, i.e. significantly far away from the protonation of py ($pK_a = 5.2$[11]) and deprotonation of B_{12}–H_2O^+ ($pK_a = 8.1$[2]). All reported kinetic measurements were therefore performed at this pH. In addition, the reactions exhibit excellent pseudo-first-order behavior (excess py), and the corresponding rate plots were linear for at least 3 half-lives of the reaction.

Results and Discussion

The observed kinetic data are summarized as a function of [py], temperature, and pressure in Table I. Under pseudo-first-order conditions, the plot of k_{obs} versus [py] (Figure 1) clearly exhibits a nonzero intercept and is significantly curved at higher [py]. The observed intercept can be assigned to the reverse aquation reaction (see further discussion), whereas the observed curvature could be evidence in favor of a limiting D mechanism. Such a curvature was also observed for the anation by CN^- [2] and was ascribed to ion-pair formation, i.e. the operation of an I_d mechanism in that system. However, in the present case ion-pair formation with a neutral ligand such as pyridine is expected to be less significant and it is questionable whether it can account for the observed curvature.

Table I. Observed Rate Constants (k_{obs},[a] s^{-1}) as a Function of [py], Temperature, and Pressure for the Reaction[b]

$$B_{12}\text{–}H_2O^+ + py \rightleftharpoons B_{12}\text{–}py^+ + H_2O$$

[py], M	temp, °C		
	20	25	37
0.01	1.30 ± 0.02	2.65 ± 0.05	9.55 ± 0.30
0.05	2.14 ± 0.05	3.95 ± 0.20	13.9 ± 1.0
0.10	2.95 ± 0.03	5.72 ± 0.05	18.7 ± 0.3
0.20		8.49 ± 0.09	
0.25	5.24 ± 0.15		31.8 ± 0.3
0.30		11.1 ± 0.05	
0.40		13.3 ± 0.2	
0.50	8.07 ± 0.20	15.0 ± 0.3	48.2 ± 3.0
1.00	12.1 ± 0.4	19.8 ± 0.5	70.2 ± 4.0

[py], M	pressure, MPa				
	5	25	50	75	100
0.01	2.40 ± 0.28	2.15 ± 0.15	1.89 ± 0.10	1.56 ± 0.07	1.30 ± 0.06
0.05	3.88 ± 0.14	3.45 ± 0.13	3.17 ± 0.14	2.75 ± 0.09	2.40 ± 0.07
0.10	5.50 ± 0.20	5.30 ± 0.15	4.77 ± 0.16	4.08 ± 0.12	3.60 ± 0.10
0.25	9.74 ± 0.50	8.89 ± 0.20	8.10 ± 0.22	7.72 ± 0.30	6.98 ± 0.32
0.50	15.3 ± 0.9	13.4 ± 0.5	13.0 ± 0.4	11.6 ± 0.5	10.4 ± 0.3
1.00	19.2 ± 0.5	17.5 ± 0.4	16.5 ± 0.3	14.6 ± 0.6	14.2 ± 0.2

[a] Mean value of at least four kinetic runs. [b] $[B_{12}\text{–}H_2O^+] = 1 \times 10^{-4}$ M; ionic strength = 0.5 M.

In terms of the limiting D mechanism outlined in (1), the observed rate law, on application of the steady-state assumption

$$B_{12}\text{–}H_2O^+ \underset{k_{-1}}{\overset{k_1}{\rightleftharpoons}} B_{12}^+ + H_2O \qquad B_{12}^+ + py \underset{k_{-2}}{\overset{k_2}{\rightleftharpoons}} B_{12}\text{–}py^+ \quad (1)$$

$$k_{obs} = \frac{k_1k_2[py] + k_{-1}k_{-2}}{k_{-1} + k_2[py]} \quad (2)$$

on the intermediate B_{12}^+ species, is given in (2). According to this expression a plot of k_{obs} versus [py] should be linear at low [py], i.e. where $k_2[py] \ll k_{-1}$, exhibit an intercept k_{-2}, and reach a limiting value of k_1 at high [py]. In addition, the initial slope of such a plot should equal k_1k_2/k_{-1}. Equation 2 can be rewritten in the form given in (3), from which it follows that a plot of $(k_{obs} - k_{-2})/[py]$ versus k_{obs} results in a straight line with slope $-k_2/k_{-1}$ and intercept k_1k_2/k_{-1}. This is indeed the case for the data in Table I, as demonstrated in Figure 2 for the data in Figure 1.

$$\frac{k_{obs} - k_{-2}}{[py]} = -\frac{k_2k_{obs}}{k_{-1}} + \frac{k_1k_2}{k_{-1}} \quad (3)$$

The data in Table I were treated in the way outlined above, and the resulting rate and activation parameters are summarized

(1) On leave from the Department of Inorganic Chemistry, Jagiellonian University, 30-060 Krakow, Poland.
(2) Reenstra, W. W.; Jencks, W. P. *J. Am. Chem. Soc.* **1979**, *101*, 5780.
(3) Lexa, D; Saveant, J. M.; Zickler, J. *J. Am. Chem. Soc.* **1980**, *102*, 2654.
(4) Balt, S.; van Herk, A. M. *Transition Met. Chem.* **1983**, *8*, 152.
(5) Balt, S.; de Bolster, M. W. G.; van Garderen, C. J.; van Herk, A. M.; Lammers, K. R.; van der Velde, E. G. *Inorg. Chim. Acta* **1985**, *106*, 43.
(6) Baldwin, D. A.; Betterton, E. A.; Pratt, J. M. *J. Chem. Soc., Dalton Trans.* **1983**, 2217.
(7) Chemaly, S. M. *J. Chem. Soc., Dalton Trans.* **1987**, 761.
(8) van Eldik, R., Ed. *Inorganic High Pressure Chemistry: Kinetics and Mechanisms*; Elsevier: Amsterdam, 1986.
(9) van Eldik, R.; Asano, T.; le Noble, W. J. *Chem. Rev.* **1989**, *89*, 549 and literature cited therein.
(10) Stochel, G.; van Eldik, R.; Kunkely, H.; Vogler, A. *Inorg. Chem.* **1989**, *28*, 4314.
(11) Perrin, D. D., Ed. *Dissociation Constants*; Butterworth: London, 1965.

0020-1669/90/1329-2075$02.50/0

Table II. Rate and Activation Parameters for the Complexation of B_{12}–H_2O^+ by Pyridine

kinetic param	method of determn	value at 25 °C	ΔH^*, kJ mol^{-1}	ΔS^*, J K^{-1} mol^{-1}	ΔV^*, cm^3 mol^{-1}
		D Mechanism			
k_1, s^{-1}	intercept/slope of eq 3	39.5 ± 5.0	78.1 ± 4.0	+48 ± 13	+7.4 ± 2.4
k_{-2}, s^{-1}	intercept of k_{obs} vs [py]	2.28 ± 0.06	86.1 ± 3.0	+50 ± 10	+16.9 ± 0.8
k_2/k_{-1}, M^{-1}	slope of eq 3	1.0 ± 0.1	−8 ± 10[a]	−273 ± 32[a]	+1.4 ± 3.6[a]
k_1k_2/k_{-1}, M^{-1} s^{-1}	intercept of eq 3	39.5 ± 1.1	72.8 ± 5.6	+29 ± 19	+8.7 ± 1.2
	slope of k_{obs} vs [py]	34.2 ± 0.9	73.0 ± 5.1	+29 ± 17	+8.7 ± 1.4
		I_d Mechanism			
k_4, s^{-1}	1/intercept of eq 6	34 ± 7	84.5 ± 2.9	+68 ± 10	+7.1 ± 1.0
k_{-4}, s^{-1}	intercept of k_{obs} vs [py]	2.28 ± 0.06	86.1 ± 3.0	+50 ± 10	+16.9 ± 0.8
K_3, M^{-1}	intercept/slope of eq 6	1.1 ± 0.2	−15 ± 7[a]	−297 ± 24[a]	+0.8 ± 1.6[a]
k_4K_3, M^{-1} s^{-1}	1/slope of eq 6	37.2 ± 0.3	71.3 ± 4.2	+24 ± 14	+8.0 ± 0.7
	slope of k_{obs} vs [py]	34.2 ± 0.9	73.0 ± 5.1	+29 ± 17	+8.7 ± 1.4

[a] These are the thermodynamic parameters ΔH°, ΔS°, and $\Delta \bar{V}$.

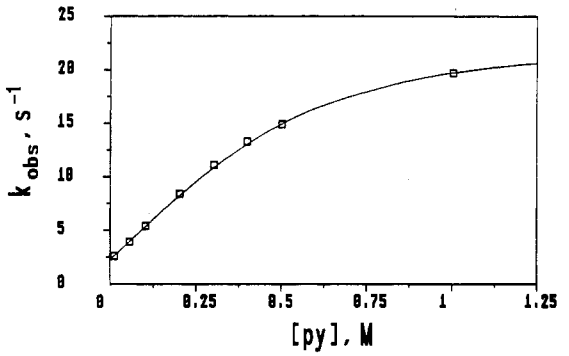

Figure 1. Plot of k_{obs} versus [py] for the reaction B_{12}–H_2O^+ + py ⇌ B_{12}–py^+ + H_2O.

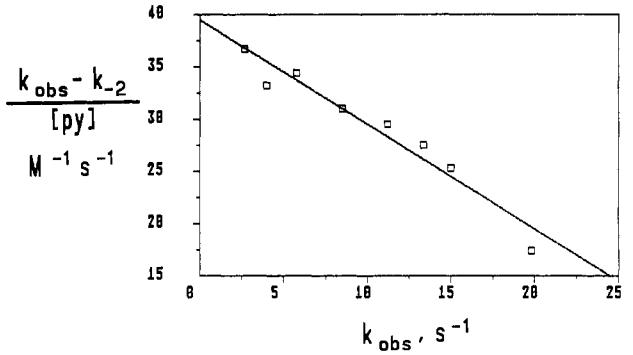

Figure 2. Plot of $(k_{obs}-k_{-2})/[py]$ versus k_{obs} according to eq 3.

in Table II. Plots of ln (kinetic parameter) versus pressure were linear within the experimental error limits in all cases and ΔV^* was calculated from the slope ($=-\Delta V^*/RT$) of such plots. The results in Table II demonstrate that the values of k_1k_2/k_{-1} and the associated activation parameters are independent of the method employed to calculate these values. Before we discuss these data, we turn to the analysis of the kinetic data in terms of an I_d mechanism, as outlined in (4). The observed rate law for this

$$\begin{aligned} B_{12}\text{–}H_2O^+ + py &\overset{K_3}{\rightleftharpoons} \{B_{12}\text{–}H_2O^+\cdot py\} \\ \{B_{12}\text{–}H_2O^+\cdot py\} &\underset{k_{-4}}{\overset{k_4}{\rightleftharpoons}} B_{12}\text{–}py^+ + H_2O \end{aligned} \tag{4}$$

mechanism, eq 5, differs slightly from that in (2) but predicts a

$$k_{obs} = \frac{k_4K_3[py]}{1 + K_3[py]} + k_{-4} \tag{5}$$

similar kinetic behavior. At low [py] it reduces to a linear relationship with slope k_4K_3 and intercept k_{-4}, whereas at high [py] a limiting rate constant $k_4 + k_{-4}$ is reached. Equation 5 can be rewritten as shown in (6), from which it follows that a plot of $(k_{obs}$

$$(k_{obs} - k_{-4})^{-1} = (k_4K_3[py])^{-1} + k_4^{-1} \tag{6}$$

$- k_{-4})^{-1}$ versus $[py]^{-1}$ should be linear with an intercept k_4^{-1} and

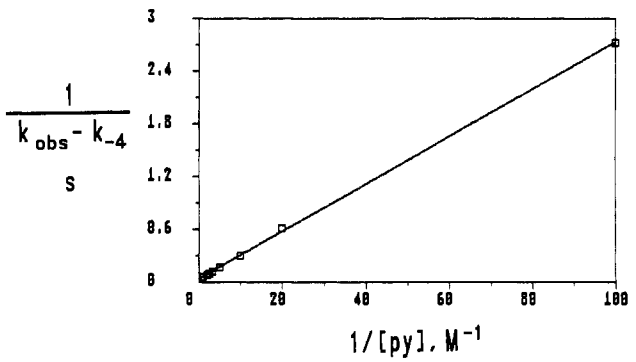

Figure 3. Plot of $(k_{obs}-k_{-4})^{-1}$ versus $[py]^{-1}$ according to eq 6.

slope $(k_4K_3)^{-1}$. This is also the case for the observed data, as demonstrated in Figure 3 for the data in Figure 1. The kinetic data (Table I) were also treated in this fashion, and the resulting rate and activation parameters are included in Table II. Once again the method used to estimate k_4K_3 has no significant influence on the data. Furthermore, rate laws 2 and 5 describe the kinetic data equally well. This is mainly due to the fact that k_{-4} (or k_{-2}) is rather small, since if (5) is rewritten as shown in (7), it reduces

$$k_{obs} = \frac{(k_4 + k_{-4})K_3[py] + k_{-4}}{1 + K_3[py]} \tag{7}$$

exactly to the same form as (2) when $k_4 \gg k_{-4}$ (see Table II). The error limits of the rate and activation parameters are influenced by the method and rate law employed to fit the data but do not affect the mechanistic interpretation. It follows that we cannot differentiate between the validity of the two possible mechanisms on the basis of the slightly different rate laws. However, a discussion of the activation parameters in terms of the suggested mechanism does enable such a differentiation.

The activation parameters (ΔS^* and ΔV^*) demonstrate the overall dissociative nature of the forward (k_1 and k_4) and reverse (k_{-2} and k_{-4}) reactions. The values of k_2/k_{-1} and K_3 exhibit no meaningful temperature and pressure dependences. This means that the volumes of activation for k_2 and k_{-1} must be very similar, which is quite acceptable in terms of the bond formation process. Similarly, the almost zero $\Delta \bar{V}(K_3)$ value is also in agreement with that expected for ion-pair formation involving a neutral reaction partner. Our main arguments to differentiate between the operation of an I_d or a D mechanism are based on the volumes of activation for k_1, k_{-2}, k_4, and k_{-4}. In the case of an I_d mechanism the interchange of H_2O for py (k_4) should be accompanied by a small positive ΔV^*.[8,9] In addition a very similar value is expected for the reverse process (k_{-4}), which should also proceed according to an I_d mechanism on the basis of microscopic reversibility. However, the value of $\Delta V^*(k_{-4})$ is too large to be accommodated in terms of an I_d mechanism. In this respect, the value of $\Delta V^*(k_{-2})$ is more in line with a limiting D mechanism. It should furthermore be significantly larger than $\Delta V^*(k_1)$, since it involves the dissociation of pyridine as compared to water ($\bar{V}$(py) = 80, $\bar{V}(H_2O)$ = 18 cm^3 mol^{-1}).[8,9] It follows that a limiting D mechanism can

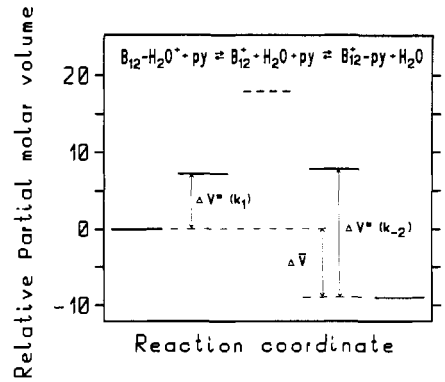

Figure 4. Volume profile for the system B_{12}–H_2O^+ + py ⇌ B_{12}^+ + H_2O + py ⇌ B_{12}–py^+ + H_2O.

better account for the observed ΔV^* data than an I_d mechanism. In addition, the curvature observed in plots of k_{obs} versus [py] results in K_3 values of ca. 1 M^{-1}, which are also too large for ion-pair formation between a 1+ and neutral species, and can therefore rather be ascribed to the operation of a D mechanism.

The interpretation of the volume of activation data in terms of a D mechanism is assisted by the construction of a volume profile diagram for the overall process outlined in (1), as shown in Figure 4. The partial molar volume of the intermediate B_{12}^+ species was predicted on the basis of a complete release of the water molecule without a significant volume collapse on the complex, i.e. a maximum volume increase of 18 cm^3 mol^{-1} during the release of H_2O in the first step of the mechanism. The overall reaction volume can be estimated from the pressure dependence of the overall equilibrium constant K ($=k_1k_2/k_{-1}k_{-2}$) or from the difference $\Delta V^*(k_1k_2/k_{-1}) - \Delta V^*(k_{-2})$ = −8.2 ± 2.0 cm^3 mol^{-1} according to the data in Table II. Combining the values of the rate constants results in a K value of 15.0 ± 0.8 M^{-1} at 25 °C. The overall equilibrium constant can also be determined from the observed spectral changes as a function of [py]. Such spectral measurements clearly indicate the operation of an equilibrium, i.e. a higher product concentration at higher [py], and the measurements at 370 nm result in a K value of 18.2 ± 1.8 M^{-1} at 25 °C and 0.5 M ionic strength, which is in excellent agreement with the kinetically determined value. This analysis also supports the interpretation of the intercept in Figure 1 in terms of a reverse aquation reaction. Furthermore, spectral measurements at 370 nm of a 5 × 10^{-5} M B_{12}–H_2O^+ and 0.2 M py solution as a function of pressure up to 150 MPa,[12] after correction for the compressibility of the solvent,[13] resulted in a reaction volume of −12.0 ± 2.0 cm^3 mol^{-1} (average value of six determinations over the pressure range 5–150 MPa). This value is again in close agreement with the reaction volume estimated from the difference in activation volumes (see above). No complications were observed during any of the kinetic or thermodynamic measurements described above that could be related to the application of pressure to the vitamin B_{12} system. Pressure denaturation of proteins usually only occurs at significantly higher pressures than applied in this study.

The volume profile clearly demonstrates the significant increase in volume during the dissociation of B_{12}–H_2O^+ (k_1) and B_{12}–py^+ (k_{-2}). The value of + 7.4 cm^3 mol^{-1} for $\Delta V^*(k_1)$ is very reasonable for a dissociative mechanism especially since we are mainly dealing with intrinsic volume changes in the absence of significant changes in electrostriction. Furthermore, this value should be significantly smaller than $\Delta V^*(k_{-2})$ on the basis of the large difference in partial molar volume of H_2O and py as mentioned above. It follows that the overall volume decrease during the substitution of H_2O by py is associated with the binding of a significantly larger ligand accompanied by the release of a smaller ligand. The fact that $\Delta V^*(k_2)$ and $\Delta V^*(k_{-1})$ are very similar in magnitude (since $\Delta V^*(k_2/k_{-1}) \approx 0$) means that very similar volume decreases must occur during bond formation of the intermediate B_{12}^+ with H_2O (k_{-1}) and py (k_2) to reach a transition state of similar partial molar volume. Not knowing the magnitude of these activation volumes makes an accurate description impossible. The observed trend can be interpreted in terms of a difference in the position of the transition state of these processes on the basis of "early" or "late" transition states.[15]

Table III. Summary of Available ΔV^* Data for the Process

$$B_{12}\text{–}H_2O^+ + L \rightleftharpoons B_{12}\text{–}L^+ + H_2O$$

L	$\Delta V^*(k_f)$, cm^3 mol^{-1}	$\Delta V^*(k_d)$, cm^3 mol^{-1}	$\Delta \bar{V}^a$	ref
N_3^-	+6.9 ± 0.2			10
$Fe^{II}(CN)_5NO^{2-}$	+8.9 ± 0.5			10
$Fe^{III}(CN)_5H_2O^{2-}$	+8.2 ± 0.8			10
$Fe^{II}(CN)_6^{4-}$	+16.2 ± 1.2			10
$SC(NH_2)_2$	+3.6 ± 0.5	+6.3 ± 2.5	−2.7 ± 3.0	16
$S_2O_3^{2-}$	+6.0 ± 0.6			16
I^-	+5.5 ± 0.8	+11.5 ± 1.6	−5.8 ± 2.3	17
py	+8.7 ± 1.2	+16.9 ± 0.8	−8.2 ± 2.0	*b*
			−12.0 ± 2.0[c]	*b*

[a] $\Delta\bar{V} = \Delta V^*(k_f) - \Delta V^*(k_d)$. [b] This work. [c] Determined spectrophotometrically.

A comparison of the available activation volume data for complex formation and reverse aquation reactions of B_{12}–H_2O^+ is presented in Table III. The values of $\Delta V^*(k_f)$ are overall values in terms of a D mechanism, i.e. $k_f = k_1k_2/k_{-1}$ according to the scheme in (1), and consist of various volume contributions. In the case of a charged entering ligand the interpretation is complicated due to solvational changes that will largely affect the observed effects.[10] On the contrary, $\Delta V^*(k_d)$ represents the activation volume for a single step, i.e. the dissociation of L (k_{-2} in (1)), and can be compared more effectively. In this case the size of the leaving group will determine the magnitude of $\Delta V^*(k_d)$, accompanied by a decrease in volume due to charge creation (increasing electrostriction) during the dissociation of B_{12}–L (L = I^-).

We conclude that all the available data underline the operation of a limiting D mechanism for the complex formation and reverse aquation reactions of aquocobalamin. The volume profile (Figure 4) reported in this paper presents an overall picture of the structural changes that occur during these processes on a volume basis. The addition of a complete set of kinetic and thermodynamic volume parameters for the reactions involving a neutral entering or leaving group has assisted the assignment of the intimate nature of the process. Finally, the results of this study demonstrate how well techniques generally developed and employed to study the mechanisms of inorganic and organometallic reactions can be applied to bioinorganic systems.

Acknowledgment. We gratefully acknowledge financial support from the Deutsche Forschungsgemeinschaft and the Fonds der Chemischen Industrie and from the Alexander von Humboldt Foundation for a fellowship to G.S.

Registry No. Aquocobalamin, 13422-52-1; pyridine, 110-86-1.

(12) Fleischmann, F. K.; Conze, E. G.; Stranks, D. R.; Kelm, H. *Rev. Sci. Instrum.* **1974**, *45*, 1427.
(13) Doss, R.; van Eldik, R.; Kelm, H. *Ber. Bunsen-Ges. Phys. Chem.* **1982**, *86*, 925.
(14) van Eldik, R. Reference 8, Chapter 3.
(15) le Noble, W. J.; Kelm, H. *Angew. Chem., Int. Ed. Engl.* **1980**, *19*, 841.
(16) van Herk, A. M. Ph.D. Thesis, Free University of Amsterdam, 1986.
(17) Hasinoff, B. B. *Can. J. Chem.* **1974**, *52*, 910.